INVESTIGATION OF LOW SALINITY WATER FLOODING BY NMR AND CRYOESEM

Hege Christin Wideroee[1], Haakon Rueslaatten[2], Tony Boassen[1], Christian M. Crescente[1], Martin Raphaug[3], Geir H. Soerland[4], Hege Urkedal[1]
[1]Statoil, Trondheim, Norway; [2]Numerical Rocks, Trondheim, Norway
[3]Quality People, Trondheim, Norway; [4]Anvendt Teknologi, Norway

This paper was prepared for presentation at the International Symposium of the Society of Core Analysts held in Halifax, Nova Scotia, Canada, 4-7 October, 2010

ABSTRACT
An experimental program was carried out to investigate the processes governing increased oil recovery obtained by low salinity water flooding. The program included the following experiments: core flooding where injected waters ionic strength and concentration of divalent ions were independently varied, Amott-Harvey wettability tests, NMR (Nuclear Magnetic Resonance) measurements, and CryoESEM (Cryogenic Environmental Scanning Electron Microscope) investigations. Berea sandstone was used as a 'model rock'. Responses in the data from low salinity flooding experiments may be attributed to wettability changes, which were supported by wettability data and NMR diffusion-T2 measurements. CryoESEM imaging confirmed that the remaining oil is associated with kaolinite, carbonate cement and 'snap-off' droplets. It is concluded that the novel combination of NMR relaxation/diffusion measurements and CryoESEM imaging is a powerful and complementary tool for detecting wettability changes.

INTRODUCTION
Low salinity water flooding is a promising new enhanced oil recovery method. The potential of the method has been demonstrated in core flooding experiments as well as in field pilots [1, 2, 3, 4]. However, there are cases where low salinity water flooding has shown no potential for increased oil recovery [5, 6].

One of the hypothesis on how flooding with diluted water mobilizes residual oil is a change in wetting conditions towards a more water wet state. There have been several explanations for this apparent change in wettability: e.g., release of oil-wet clay particles to the pore fluids [1]; expansion of the electric double layer followed by removal of organo-metallic complexes and organic components due to ion exchange with uncomplexed cations when salinity decreases [2, 7]; desorption of oil attached to the pore surfaces due to expansion of the electric double layer [8]; and an increased pH close to the pore surface [9]. Vledder *et al*. [10] claim to have proven wettability alteration from oil-wet to water-wet on field scale. However, the understanding of the mechanisms of increased oil recovery by low salinity water flooding is still evolving.

The purpose of this study is to combine a variety of complementary experimental data in order to investigate the mechanisms governing increased oil recovery by low salinity water flooding.

We investigate the apparent changes in wettability using a novel combination of NMR transverse relaxation (T2) and diffusion measurements and visualization of fluid distribution at pore scale by CryoESEM. Measurements of NMR relaxation, apparent diffusion coefficient (ADC), and combinations of these are widely used for the characterization of porous media and the distribution of fluids therein. The sensitivity of particularly the water T2 towards contact with the pore surface makes NMR an attractive tool in wettability analysis. Studies employing diffusion-T2 measurements, where the potentially overlapping oil and water T2 signals may be resolved in the diffusion dimension, have demonstrated the potential of this method for the evaluation of wettability changes [11, 12, 13]. Studies of fluid distribution at pore scale were previously performed by Cryo SEM [14, 15]. However, this technique requires a coating film on the sample surface to obtain electric conductivity, which is not required with the ESEM. The elemental distribution is analyzed by EDS X-ray analyses [16, 17].

EXPERIMENTS

Core flooding experiments are performed to investigate the effect of increased oil recovery by tertiary low salinity flooding (varying both the ionic strength and concentration of divalent ions). Complementary experiments are Amott/USBM wettability, NMR analyses and CryoESEM imaging.

Rock Samples and Fluids

Core plugs of Berea sandstone were used. Prior to experiments, they were cleaned in toluene and methanol. Petrography was based on SEM analyses of thin sections from end cuts of the plugs, see composition in Table 1. The grain size is varying from fine to medium sand. Quartz is the dominant mineral, while feldspars constitute a minor fraction of the sand. Remnants of dissolved feldspars indicate that they are the major source of the clay content in the rock. This can also explain the patchy distribution of the clay; particularly the kaolinite, which is the dominant clay mineral in the rock. Iron-bearing carbonate cement is also seen in the thin sections (Figure 5a). Two rock samples were selected to investigate the composition of clays confined in the pore system. The fine fraction (<4 μm) was separated out and analyzed on an X-ray diffractometer (Table 1). Besides the dominant kaolinite fraction, a rather high content of illite is measured. However, diagenetic (pore lining) illite and chlorite are not observed in the SEM images but are suggested to be part of the small clay clasts. He-porosity of the core plugs ranges from 18 to 21% and water permeability ranges from 133 to 302 mD (Table 4).

Oil from a Norwegian offshore oil field (Table 3) was used for this study. The oil has been degassed, stabilized at 85^{o}C and filtered through a 1.4 μm filter. The waters were prepared from distilled water and reagent grade chemicals (Table 2), and subsequently evacuated to remove dissolved gases.

Core Preparation

Each core plug was initially saturated with SFW (Table 2). Initial water saturation was obtained by centrifuging, except for plug BE9, which was drained by porous plate. The core plugs were aged for three weeks at 85°C and ambient pressure (Table 4).

Experiments

Wettability

The wettability of the systems rock/oil/SSW1 and rock/oil/LSW1 were measured by Amott Harvey/USBM wettability tests (Table 4).

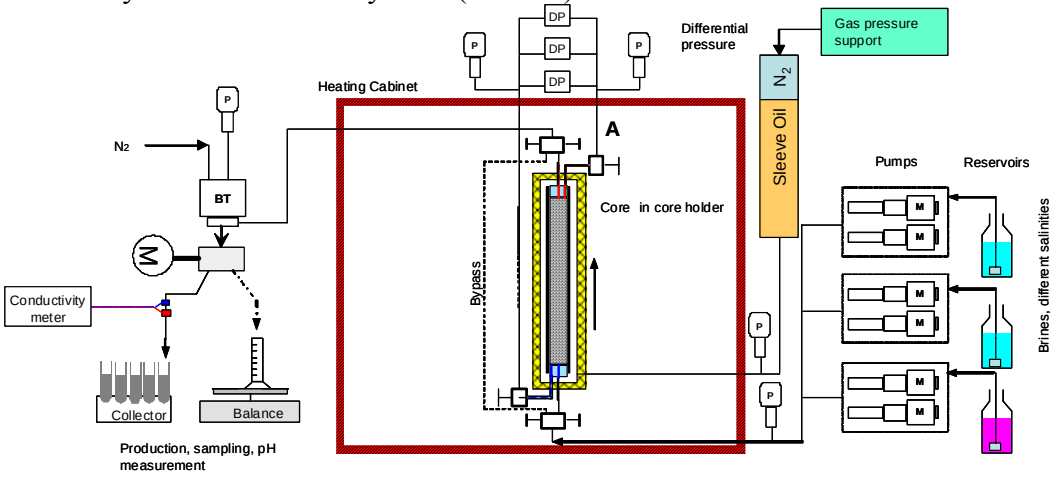

Figure 1 Experimental setup of flooding experiments.

Flooding Experiments

Figure 1 shows the experimental setup for the flooding experiments. The temperature was 60°C, sleeve pressure 60 bar, and the back-pressure 20 bar. Conductivity was measured directly in the flow line behind the back pressure (BP) valve, and pH was measured in effluent samples collected in test tubes in a carrousel. Samples were capped immediately to avoid pH change from evaporation and contact with air.

Flooding of core BE9 was performed by injecting SSW1 at 16 ml/h. One-phase experiments showed no clay production at this rate. The next floodings were SSW2, LSW1, LSW2, LSW3 and LSW4. After flooding, the core was frozen for CryoESEM analysis. Differential pressure (DP) and conductivity were recorded continuously, and the effluents were monitored in a sample collector. The conductivity measured here is not measured using a standard but shows the relative conductivity in each floodings. These measurements were used to monitor the displacement of the various salinity waters.

The core studied by NMR (BE6) was flooded by SSW1, LSW1, LSW2 and LSW4. Between each flooding the core was dismounted and analyzed by NMR. In this core and the ones used for CryoESEM (BE1 to BE5) the flooding rate was 8 ml/h. CryoESEM is a destructive method and five parallel cores were flooded in the same sequence used for the NMR study but stopped at the following stages: Swi, aging, SSW1, LSW1 and LSW2.

NMR Experiments

Each step in the flooding sequence of BE6 was followed by NMR analyses: measurements of T2, diffusion, and diffusion-T2 correlation (D-T2). The NMR system comprises a Maran DRX 12 MHz spectrometer (at 30°C), equipped with a gradient coil delivering up to 225 G/cm. The D-T2 measurements were conducted by combining the bipolar Pulsed Field Gradient Spin Echo (PFGSE) method [18] and the Carr-Purcell-Meiboom-Gill (CPMG) experiment [19, 20, 21]. In the CPMG part of the sequence a τ=150 μs was used, the combined PFGSE-CPMG experiment the gradient pulse length was set to 2.4 ms, and the eddy current delay to 0.4 ms. With these settings the transient magnetic fields following the gradient pulses had no significant effect on the echo attenuation. A time interval of 0.1 ms was used between the initial $\pi/2$ pulse and the following gradient pulse, giving a τ' value of 2.9 ms in the PFGSE part of the sequence, and a total time of 11.6 (= 4 times τ') ms before the start of the CPMG measurement.

CryoESEM imaging

The core samples were frozen in liquid nitrogen immediately after dismounting from the core holders. The cores were disintegrated into several sample chips and trimmed in frozen condition to approximately 1cm^3 to fit the cryo sample holder. In the cryo chamber, the samples were split (freeze fractured) under vacuum conditions to avoid ice crystal growth. Analyses were performed at cryo holder temperatures below -100°C.

RESULTS

Wettability

The changes in remaining oil after spontaneous imbibition in sea water (SSW1) and low salinity water (LSW1) are given in Table 4. The two plugs exposed to the low salinity water imbibed most water and show the highest Amott Wettability Indices. This is in line with published hypotheses and results [1, 2, 8].

Flooding

The SSW1 flooding of all plugs gave a remaining oil saturation ranging from 0.28 to 0.41 (Table 4). The subsequent floodings with LSW1, LSW2, LSW3 and LSW4 gave a reduction in remaining oil saturation of 0-3%. Despite no extra oil recovery from some of the core plugs, there were responses in DP, ion concentration and pH (Figure 3). For LSW4, a significant DP increase was observed only in the long core, the short cores had minor DP increase and decrease. Clay minerals were not observed in the effluents.

Flooding data of BE9

SSW1 flood: The DP and production data from the SSW1 flooding were history matched. See match in the SSW1 part of Figure 3a and estimated functions in Figure 2.

SSW2 flood: SSW2 was injected to study the effect of exchanging divalent with mono-valent ions. Ion analysis of the effluent water shows a gradual decrease in divalent cations. The pH increases correspondingly. There is a DP declined due to an unfortunate pump stop. The DP did not resume the previous level.

LSW1 flood: DP increases while SSW2 is replaced by LSW1 and stabilizes. Fluid replacement is also observed in conductivity data. The concentration of Ca^{2+} and Mg^{2+} drops far below the LSW1 concentration (i.e., a salinity shock) and pH increases.
LSW4 flood: DP increases with low ionic strength in injected water and high pH.

NMR Measurements
NMR T2 relaxation distributions of BE6 at each stage are shown in Figure 4. The T2 distribution at 100% water saturation is included in all the subplots for reference, and the D-T2 contour plots are overlain their respective T2 distributions. For the two first stages (at Swi) only the oil signal is visible in the D-T2 plots. This is due to the experimental setup for the diffusion measurements, which includes a limitation with respect to detecting the fastest relaxing components, i.e. clay bound water. However, these signals are seen in the CPMG relaxation distribution.

Before and after Ageing: The three peaks constituting the oil signal at Swi before ageing (Figure 4a) appear similar to the bulk oil response, as expected for a water wet state. The broad range in the ADC and T2 relaxation corresponds to the complex composition of the crude oil. After ageing, the main peak in the T2 distribution shifts towards slightly shorter T2 value, and a similar small shift is seen for the three oil peaks in the D-T2 plot, indicating some surface relaxation of the oil.
SSW1 flood: After the SSW1 flooding, the water signal appears in the D-T2 plot at an ADC around that of bulk water, at 2.9×10^{-9} m^2/s. The water peak extends to higher T2 values than the one at 100% water saturation, indicating less contact with the rock surface. This is confirmed by the T2 distribution, which also shows a small amount of water relaxing as bulk water, manifested by a peak at 1-3 seconds (Figure 4c). The longer T2 suggests that the less water-wet state obtained after ageing was, at least partly, preserved during the SSW1 flooding. The oil signal was significantly reduced after SSW1 flooding and the peaks shifted to shorter T2 values. With the lower oil signal the uncertainty in the ADC increased. The leftmost oil peak is on the detection limit.
LSW1 flood: After the LSW1 flooding, the peak at 1-3 seconds disappeared on the T2 distribution (Figure 4d), indicating increased water surface relaxation, which means a stronger water-wet behaviour. This is confirmed by D-T2, where the water signal has moved to shorter relaxation times. Furthermore, the water peak extends towards the oil peaks; i.e. with ADCs slower than the main peak. These features were maintained in the subsequent floodings. The rightmost oil peak extends towards faster ADCs and longer T2 times compared to what is seen in Figure 4c.
LSW2 flood: The LSW2 flooding brought back the slow relaxing peak at 1-3 seconds, seen both in the T2 distribution and in the D-T2 plot (Figure 4e). Also, the bulk of the water signal shifted to slightly higher T2 value. The flooding was not accompanied by any saturation change.
LSW4 flood: Finally, the LSW4 flooding resulted in similar changes in the water response as after the LSW1 flooding. The water peak at 1-3 seconds was reduced and the main water peak shifted to shorter relaxation times, indicating increased water surface relaxation; i.e., a more water-wet state (Figure 4f).

The NMR experiment was repeated on a new plug, with similar trends in T2 relaxation.

CryoESEM Imaging
CryoESEM imaging was carried out to visualize the fluid distribution in the pore system after flooding with SSW1, LSW1 and LSW2. An overview of the complex distribution of oil and water in the pore system of BE5 after LSW2 flooding is shown in Figure 5b. Residual oil is found both as 'snap-off' droplets and as oil blobs associated with mineral surfaces (Figures 5b and c). A substantial amount of oil is associated with clays, mainly kaolinite, and iron-rich carbonate cement (Figures 5b, d and f). The CryoESEM images of BE3 to BE5 do not show any significant differences in fluid distribution and saturation between the floodings with SSW1, LSW1 and LSW2. The CryoESEM images of BE9 show more oil as 'snap-off' droplets compared to BE5 (Figure 5b and c).

A quantitative image analysis of saturation requires flat, polished surfaces that represent an elementary volume of the rock. Such surfaces are difficult to obtain with the existing preparation technique. However, a semi quantitative image analysis can be done on samples having minor topography. Oil and water areas are identified, and the oil saturation is calculated by $So=\Sigma Area_{oil}/\Sigma Area_{oil+water}$. The oil saturations calculated from CryoESEM are in line with the oil gradient estimated from BE9 flooding data (estimated saturations are So=0.24 at inlet and So=0.44 at outlet).

DISCUSSION
The cores responded to low salinity waters, both in DP, ion concentration and pH. Since no clay minerals were observed in the effluent, the change in DP may be explained by changes in rock-fluid or fluid-fluid interactions due to processes initiated by low salinity waters, e.g. a wettability change towards more water wet (a sensitivity study shows that a 10% decrease in water relative permeability matches the pressure response in LSW1).

The pH responses show that chemical reactions take place when low salinity water replaces the higher salinity water in the core. For LSW1 it seems to be a cation exchange, i.e., the very low ion concentration (shock) and corresponding high pH may be due to the chromatographic effect.

However, the reduction in oil saturation by low salinity waters was very small for this batch of Berea samples. Both the capillary end effect and the lower rate (compared to the long core) can explain the higher remaining oil saturation in the short cores. Consequently, the short cores had more mobile oil and showed some response to low salinity waters. The lack of response in the long core may be due to insufficient mobile oil or that low salinity flooding is not an effective method for the state of this rock/oil/water system. Oxidation of the Berea has also been suggested as a cause [22].

Parallel to the flooding program, studies on NMR and CryoESEM were ongoing to validate subtle variations in wettability. It is suggested that the changes in the NMR diffusion coefficients after low salinity floodings reflect the partitioning of polar oil

components into the low salinity water phases. Furthermore, it is suggested that these components are associated with the apparent wettability changes, due to interaction with clay minerals in particular. The water-oil interaction may influence on the NMR responses for both oil and water. The wettability changes (inferred from NMR data) may well be due to adsorption/desorption processes, where metal-organic complexes and positively charged organic components are interacting with clay mineral surfaces.

The CryoESEM images of BE5 after flooding with SSW1 and LSW2 show a higher amount of oil associated with kaolinite compared to BE9. In BE5 oil is filling small pores within the clay, which would have too high capillary entry pressure for the oil to enter if they were water-wet. Since the Swi=0.08 for BE5 and Swi=0.15 for BE9, the different methods to establish Swi may have caused more oil to contact the rock/clay surface in BE5 compared to BE9. Hence, this clay-bound oil may have been mobilized.

CONCLUSIONS

- Wettability tests of Berea indicate stronger water wetness with low salinity water.
- NMR diffusion and T2 observations indicate an apparent wettability change after low salinity water flooding. Diffusion measurements suggest that polar oil components are partitioning from the oil into the water.
- CryoESEM analyses show the fluid distribution in the pore system, and indicate the wetting properties of the different mineral surfaces. A majority of the residual oil is found as ‘snap-off’ droplets and associated with clay and carbonate cement.
- Clay minerals are not observed in the effluents, however, flooding of water with low ionic strength and high pH may give an increase in DP.
- The combined use of flooding data, NMR and CryoESEM is regarded as a powerful tool for investigating low salinity flooding effects on core material.

ACKNOWLEDGEMENTS

We would like to thank Medad Tweheyo and Kaare Solbakken for valuable input to this work. Thanks to Statoil for permission to publish this material.

REFERENCES

1. Tang, G.Q., Morrow, N.R.: “Influence of brine composition and fines migration on crude oil/brine/rock interactions and oil recovery,” *J. of Petroleum Science and Eng.* (1999) **24**, 94-111.
2. Lager, A., Webb, K.J, Black, C.J.J., Singleton, M., Sorbie, K.S.: “Low salinity oil recovery: An experimental investigation,” *Int. Symp. of the Society of Core Analysts*, Trondheim (12-16 Sept., 2006).
3. McGuire, P.L., Chatham, J.R., Pahvan, F.K., Sommer, D.M., Carini, F.H.: “Low salinity oil recovery: An exciting EOR opportunity for Alaska’s North Slope;” *SPE 93903* (March 2005).
4. Seccombe, J.C., Lager, A., Jerauld, G., Jhaveri, B., Buikema, T., Bassler, S., Denis, J., Webb, K., Fueg, E.S.: “Demonstration of low-salinity water EOR at interwell

scale, Endicott field, Alaska," *SPE 129692, presented at the 17th SPE IOR Symp.*, Tulsa, OK. (April 24-28, 2010).
5. Sorbie, K.S., Collins, I.: "A proposed pore-scale mechanism for how low salinity waterflooding works," *SPE 129833 presented at the 17th SPE IOR Symp.*, Tulsa, OK. (April 24-28, 2010).
6. Skrettingland, K., Holt, T., Tweheyo, M.T., Skjevrak, I.: "Snorre low salinity water injection - core flooding experiments and single well field pilot," *paper SPE 129877 presented at the 17th Symp. on IOR,* Tulsa, Oklahoma (24-28 April, 2010).
7. Lee, S.Y., Webb, K., Collins, I., Lager, A., Clarke, S., O'Sullivan, M., Routh, A., Wang, X.: "Low-salinity oil recovery: Increasing understanding of the underlying mechanisms," *paper SPE 129722 presented at the 17th Symposium on IOR,* Tulsa, Oklahoma (24-28 April, 2010).
8. Ligthelm, D.J., Gronsveld, J., Hofman, J.P., Brussee, N.J., Marcelis, F., van der Linde, H.A.: "Novel Waterflooding Strategy by Manipulation of Injection Brine Composition", *paper SPE 119835, SPE Annual Conf. and Exhib.*, Amsterdam, The Netherlands (8-11 June, 2009).
9. Austad, T., Rezaeidoust, A., Puntervold, T.: "Chemical mechanism of low salinity water flooding in sandstone reservoirs", *paper SPE 129767, proceedings SPE IOR Symp.*, Tulsa, Oklahoma (24-28 April, 2010).
10. Vledder, P., Fonseca, J.C., Wells, T., Gonzalez, I., Ligthelm, D.: "Low-salinity water flooding, proof of wettability alteration on a field-wide scale," *paper SPE 129564 presented at the 17th Symposium on IOR,* Tulsa, Oklahoma (24-28 April, 2010).
11. Freedman R., Heaton N., Flaum M., Hirasaki G.J., Flaum C., Hürlimann M.: "Wettability, saturation, and viscosity from NMR measurements," *SPE 87340, SPE Journal* (December 2003).
12. Flaum M., Chen J., and Hirasaki G.J.: "NMR diffusion editing for D-T2 maps: Application to recognition of wettability change," *Petrophysics* (2005) **46**: 113-123.
13. Toumelin, E., Torres-Verdín, C., Sun, B., Dunn, K.-J.: "Limits of 2D NMR interpretation techniques to quantify pore size, wettability, and fluid type: A numerical sensitivity study," *SPE 90539, paper presented at the SPE Ann. Tech. Conf. and Exhib.*, Houston (26-29 Sept., 2004).
14. Sutanto, E., Davis, H.T. and Scriven, L.E.: "Liquid Distribution in Porous Rock Examined by Cryo Scanning Electron Microscopy," *paper SPE 20518 presented at the SPE Ann. Tech. Conf. and Exhib.,* New Orleans (23-26 Sept., 1990).
15. Rueslatten, H., Oeren, P-E., Robin, M., Rosenberg, E. And Cuiec, L.: "A combined use of Cryo-SEM and NMR-Spectroscopy for studying the distribution of oil and brine in sandstones," *paper SPE 27804 presented at the SPE/DOE 9th Symp. on IOR,* Tulsa (17-20 April, 1994).
16. Kowalewski, E., Boassen, T., Torsaeter, O.: "Wettability alterations due to aging in crude oil; wettability and Cryo-ESEM analyses," *J. of Pet. Sci.and Eng.* (2003) **39**: 377-388.
17. Boassen, T., Kowalewski, E., Hemmingsen, P.V.: "Cryo ESEM studies of emulsions and fluid distribution at pore scale," *Int. Symp. of the Society of Core Analysis*, Trondheim (12-16 Sept., 2006).

18. Soerland, G.H., Aksnes, D., and Gjerdaker, L.: "A pulsed field gradient spin echo method for diffusion measurements in the presence of internal gradients," *J. Magnetic Resonance* (1999) **137**: 397-401.
19. Carr, H.Y., Purcell, E.M.: "Effect of diffusion on free precession in nuclear magnetic resonance experiments," *Physical Review* (1954) **94**: 630-638.
20. Meiboom, S., Gill, D.: "Modified spin-echo method for measuring nuclear relaxation times," *Rev. Sci. Instrum* (1958) **29**: 688-691.
21. Seland, J.G., Soerland, G.H., Anthonsen, H.W., Krane, J.: "Combining PFG and CPMG NMR measurements for separate characterization of oil and water simultaneously present in a heterogeneous system," *Applied Magnetic Resonance* (2003) **24**: 41-53.
22. Zhang, Y., Morrow, N.R.: "Comparison of secondary and tertiary tecovery with change in injection brine composition for crude oil/sandstone combinations," *SPE 99757, SPE/DOE Symp. on Improved Oil Recovery*, Tulsa, OK (April 2006).

TABLES AND FIGURES

Table 1 Semi-quantitative X-ray diffraction analysis: Left: Bulk (average of six Berea samples and thin section/SEM). Right: Fine fraction < 4µm (average of two Berea samples).

Sample	Quartz	Kfsp+Carb	Clays	Fe-Carb	IA Poro
Berea	68.1	3.4	11	0.3	17.2

Sample	Quartz	Kfsp	Chl	Kaol	Ill	ML	Carb
Berea	5.2	2.3	3.2	59.6	26.7	2.4	0.5

Kfsp=K-feldspar; Chl=Chlorite; Kaol=Kaolinite; Ill=Illite; ML=Mixed Layer Clay; Fe=Iron; Carb=Carbonate; IA=Image Analysis.

Table 2 ID and composition and waters.

Water ID	Type of water	ppm TDS	Ionic strength	Divalent ions
SFW	Synthetic formation water	64 568.0	1.156	3.7 %
SSW1	Synthetic sea water	34 822.0	0.690	4.9 %
SSW2	Synthetic sea water, no divalent ions	40 398.0	0.691	0.0 %
LSW1	Diluted SSW1	2 089.0	0.041	4.9 %
LSW2	Diluted SSW1	348.0	0.007	4.9 %
LSW3	Diluted SSW2	2 424.0	0.041	0.0 %
LSW4	Diluted SSW2	405.0	0.007	0.0 %

Table 3 Oil properties.

Property	Oil
TAN [mg/g]	2.69
TBN [mg/g]	0.85
Wax content [mg/g]	27.28
Asphalthenes [wt%]	6.5

Table 4 Core properties and remaining oil saturations after wettability test and flooding.

Exp.	Sample	Porosity [frac.]	Core Length [cm]	Perm. Kw[mD]	Swi	So (Spont. imb)	So (Forced imb.)	Wett. Index
Wettability	BE1_1	0.20	4.80	226	0.13	0.43	0.32	0.79
	BE1_2	0.20	4.80	236	0.12	0.42	0.30	0.80
	BE1_3	0.20	4.80	302	0.14	0.39	0.31	0.85
	BE1_4	0.21	4.80	297	0.14	0.34	0.27	0.89

Exp.	Sample	Porosity [frac.]	Core Length [cm]	Perm. Kw[mD]	Swi	So (SSW1)	So (SSW2)	So (LSW1)	So (LSW2)	So (LSW3)	So (LSW4)
CryoESEM	BE1	0.19	4.8	166	0.09						
	BE2	0.21	4.8	336	0.13						
	BE3	0.18	4.8	133	0.10	0.36					
	BE4	0.19	4.8	144	0.10	0.35	-	0.34			
	BE5	0.19	4.8	179	0.08	0.42	-	0.41	0.41		
NMR	BE6	0.19	4.0	152	0.08	0.38	-	0.36	0.36	-	0.35
Flood	BE9	0.20	28.0	223	0.15	0.28	0.28	0.28	-	0.28	0.28

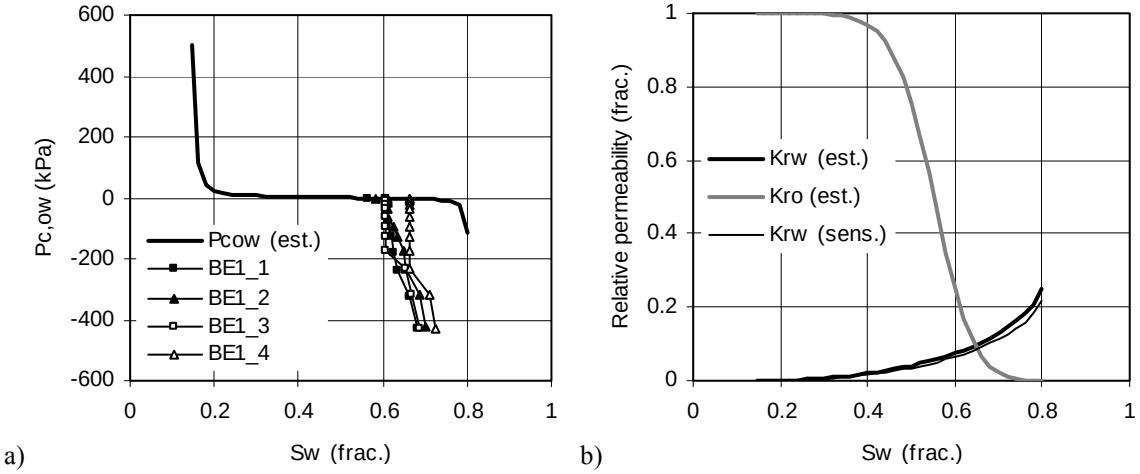

Figure 2 a) Capillary pressure from forced imbibition (centrifuge) and estimated capillary pressure from BE9 flooding data. b) Estimated relative permeability from BE9 flooding data (by history matching).

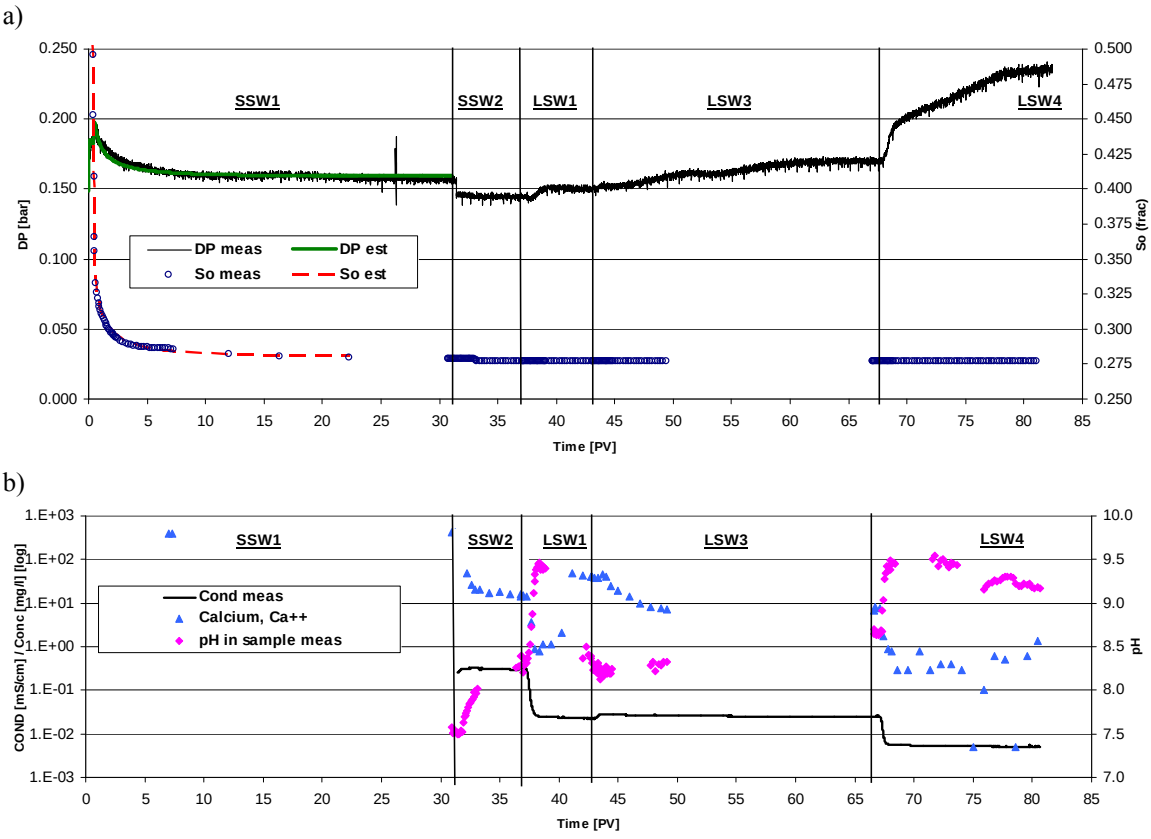

Figure 3 Experimental data from flooding of BE9 (flooding sequence SSW1, SSW2, LSW1, LSW2, LSW4). There is a pressure decline in SSW2. This is due to an unfortunate pump stop. The DP did not resume the previous level. a) DP and oil production data. The data for step SSW1 are history matched. b) Conductivity, concentration of Ca^{2+} ions, and pH data.

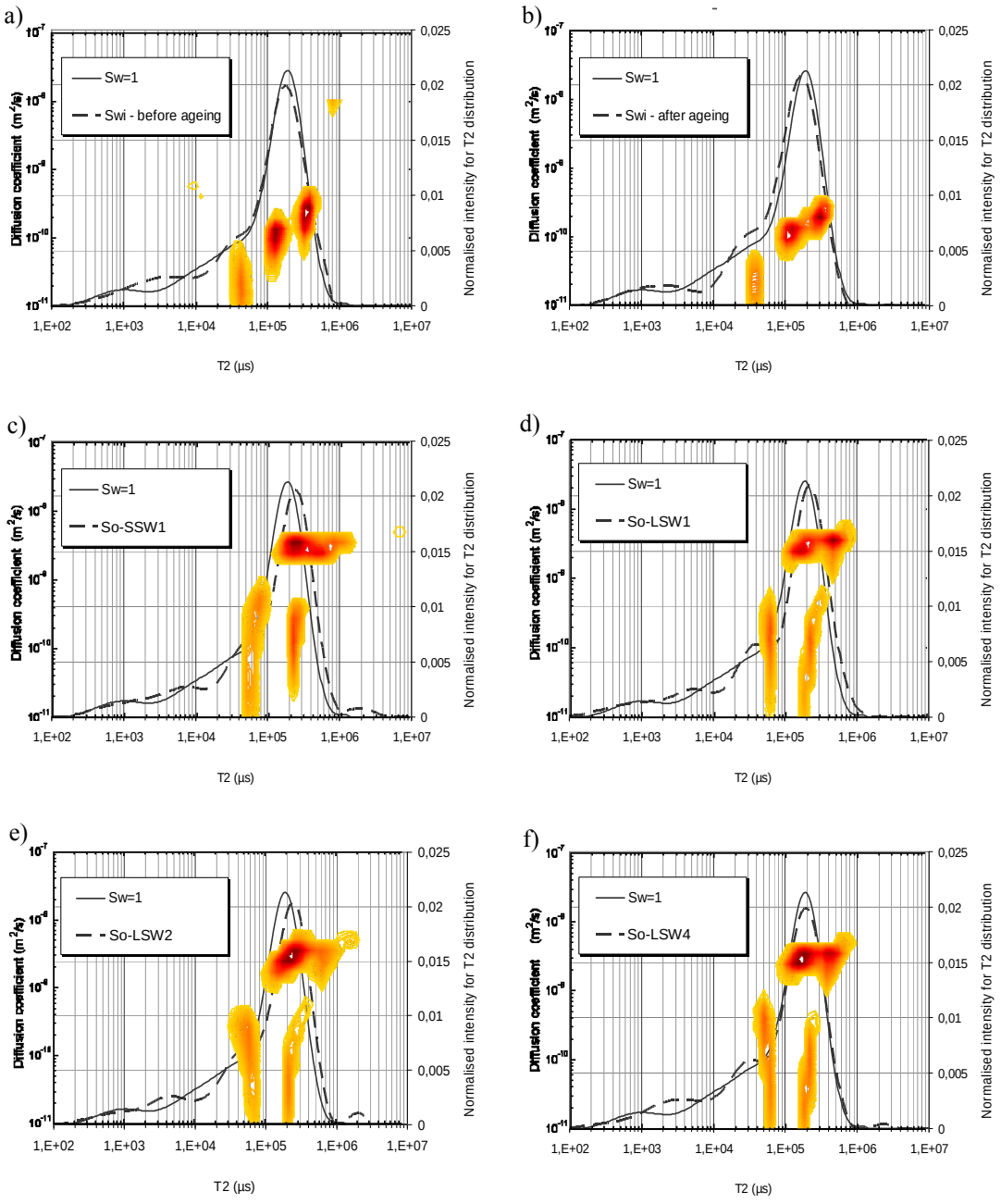

Figure 4 T2 distributions of the water saturated plug plotted together with T2 distributions and diffusion-T2 plots (orange blurs/contours) at a) Swi before ageing, b) Swi after ageing, c) Remaining oil saturation after SSW1 flood, d) Remaining oil saturation after LSW1 flood, e) Remaining oil saturation after LSW2 flood, and f) Remaining oil saturation after LSW4 flood.

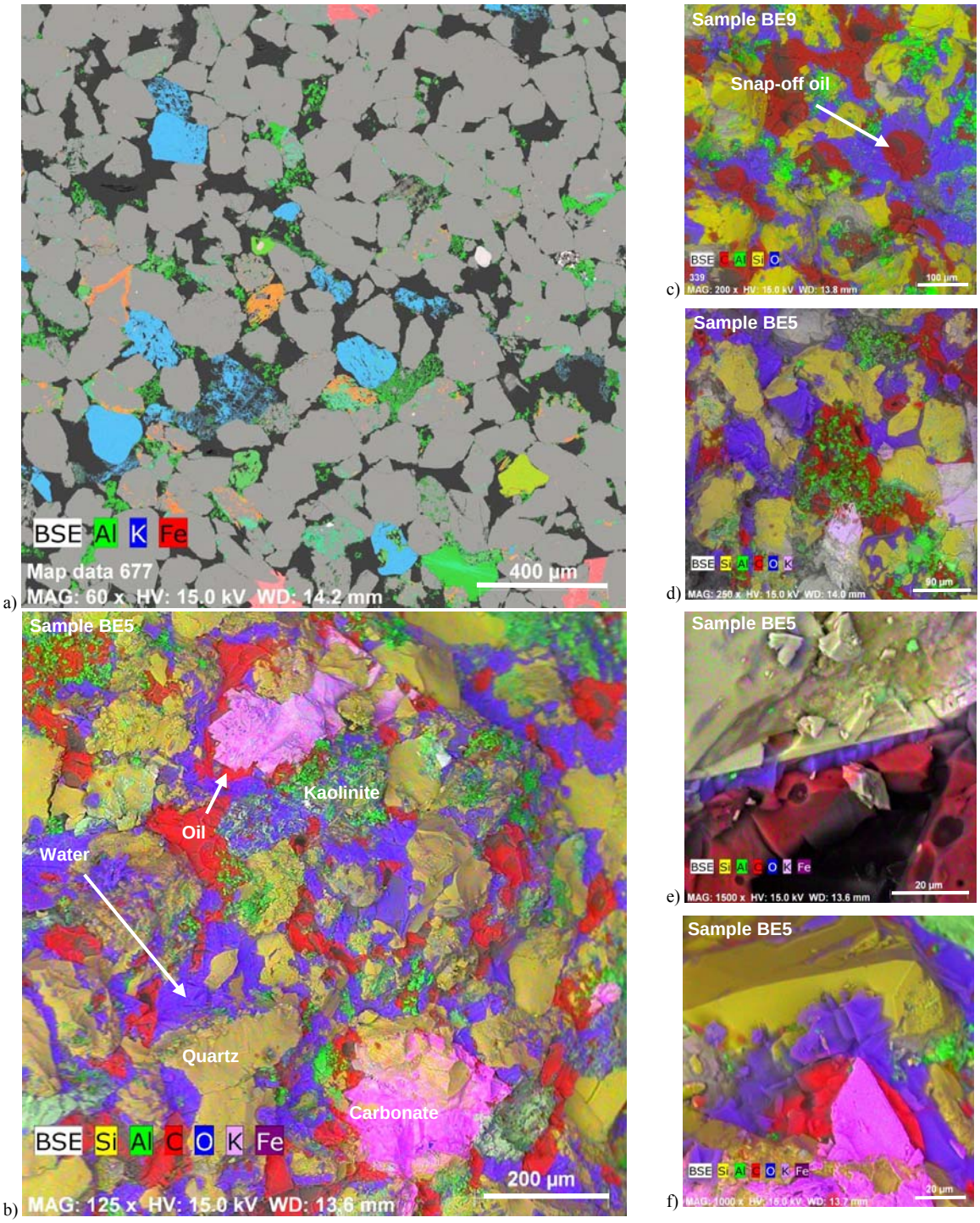

Figure 5 a) BSE image/X-ray image of thin section. b) CryoESEM image showing the distribution of oil (red) and water (blue) after flooding with LSW2 (BE5). 'Snap-off' oil is commonly seen in this strongly water-wet rock, but residual oil is also seen associated with partly oil-wet kaolinite (green) and iron-rich carbonate cement (purple). Quartz (yellow) grains are largely water-wet.
c) CryoESEM image from BE9. Oil is less associated with clay, mostly 'snap-off' oil. The oil saturation is less than in image b).
d) Oil associated with Kaolinite. e) Oil, water and quarts. f) Oil wet carbonate, water wet quarts.